A Generic Method for Retrieval of Aerosol over Land from Passive Optical Remote Sensing Data

Eric Vermote

NASA Goddard Space Flight Center Code 619

Eric.f.vermote@nasa.gov

International Meeting on Air Pollution in Asia, Inventories, Monitoring and Mitigation, February 1-3, Hanoi, Vietnam

A Land Climate Data Record

Multi instrument/Multi sensor Science Quality Data Records used to quantify trends and changes

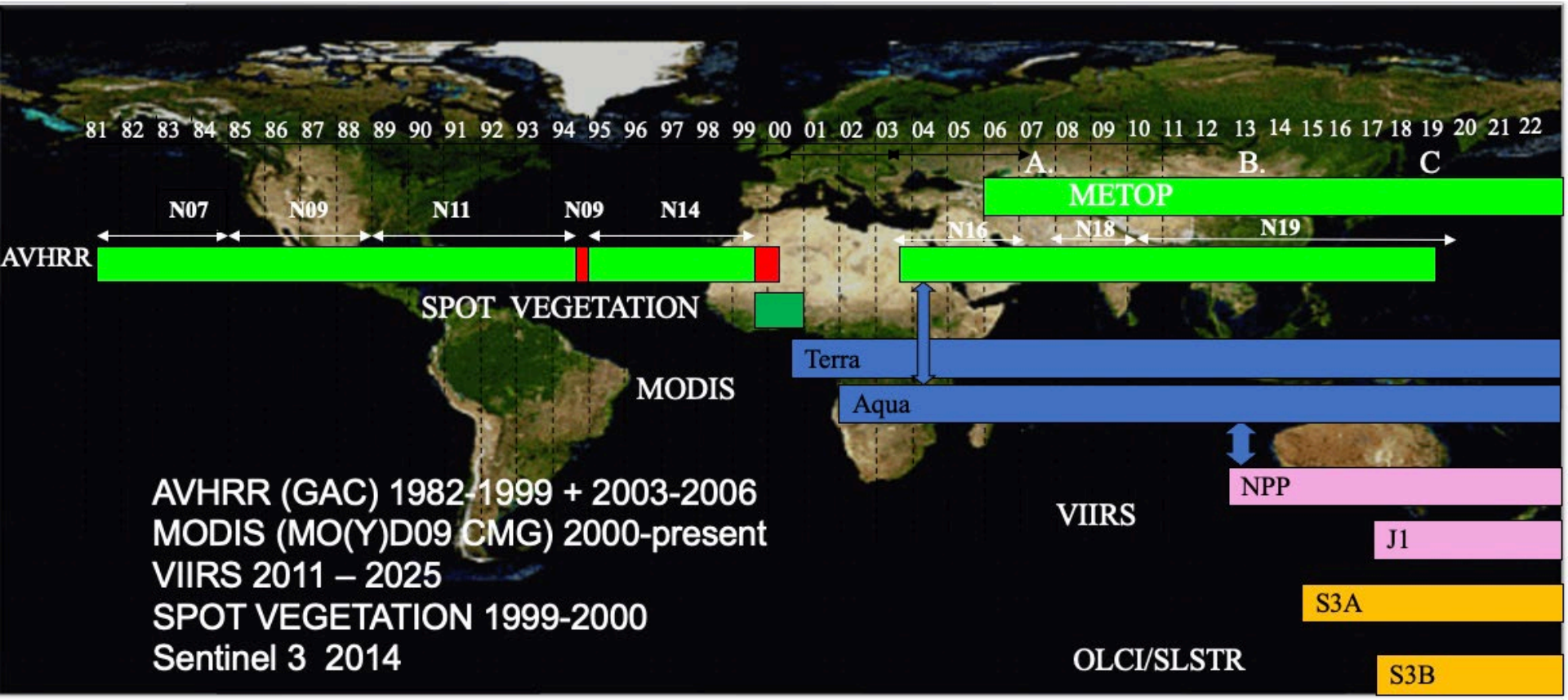

https://ltdr.modaps.eosdis.nasa.gov

Emphasis on data consistency – characterization rather than degrading/smoothing the data

Land Climate Data Record (Approach)

Needs to address geolocation,calibration, atmospheric/BRDF correction issues

CALIBRATION

Degradation in channel 1
(from Ocean observations)

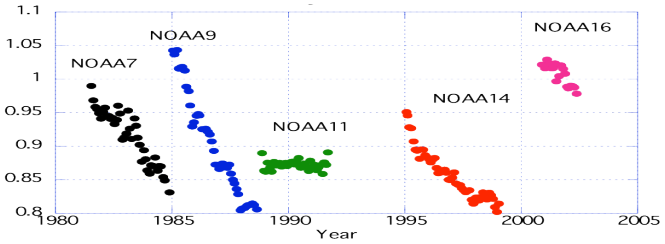

Channel1/Channel2 ratio
(from Clouds observations)

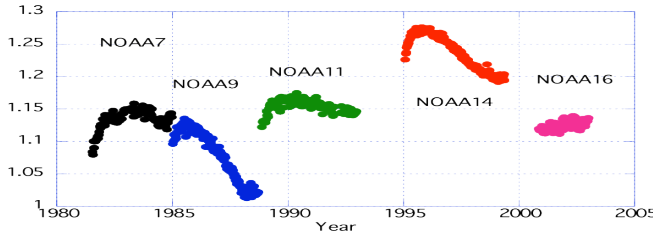

ATMOSPHERIC CORRECTION

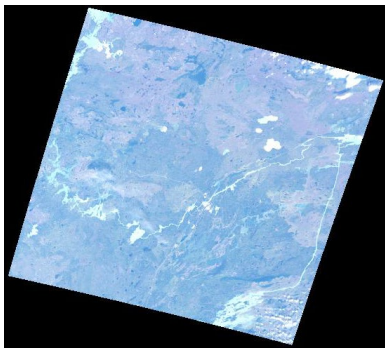

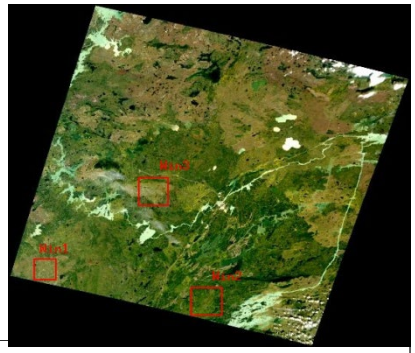

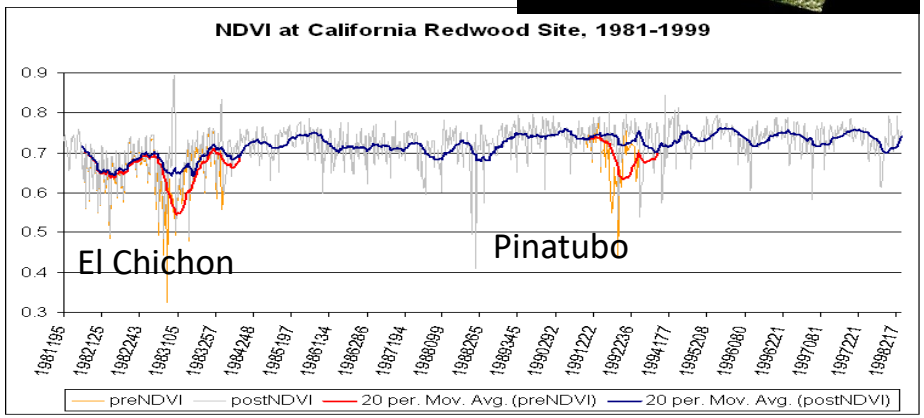

BRDF CORRECTION

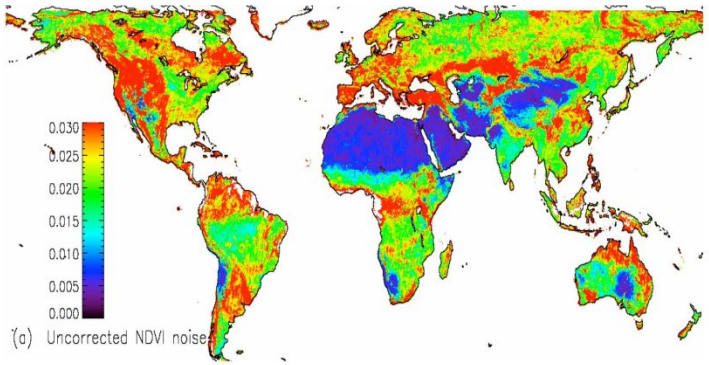

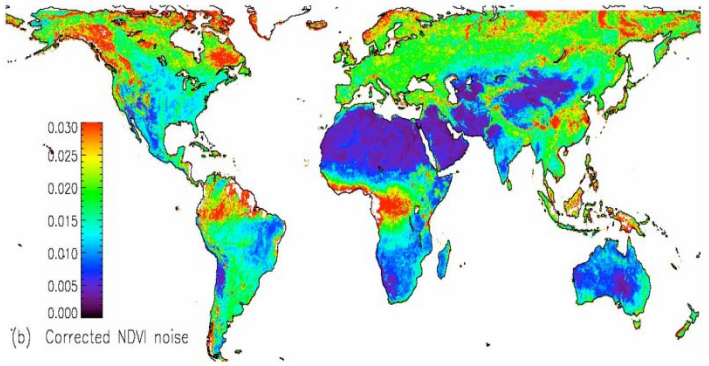

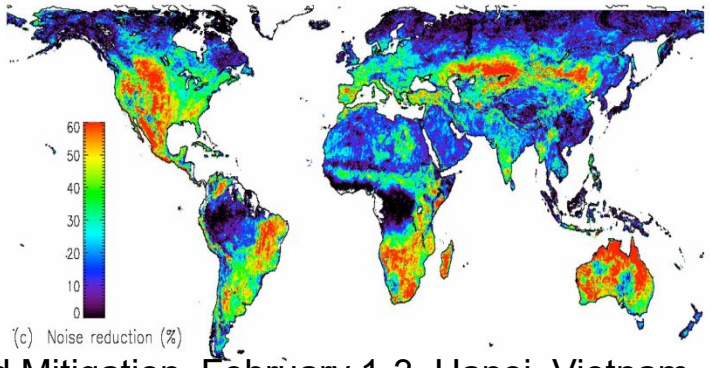

AVHRR THE URGE FOR ATMOSPHERIC CORRECTION

Mount Pinatubo eruption 1991 second largest in 20h century

Stratospheric AOT from AVHRR

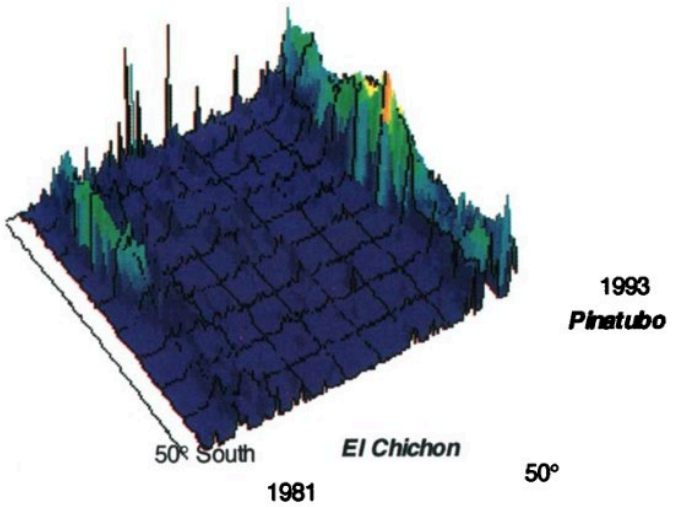

Plate 2. Monthly average of the stratospheric aerosol optical depth deduced from the advanced very high resolution radiometer (AVHRR) data showing major eruptions of El Chichon (1982) and Pinatubo (1991).

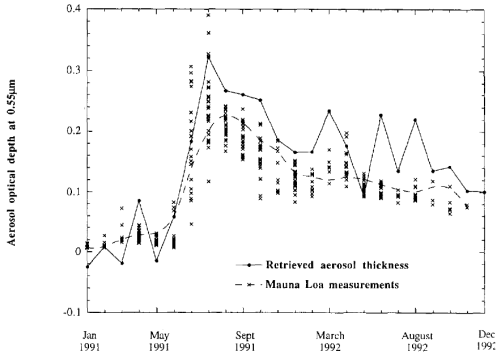

FIGURE 4 Comparison between retrieved "stratospheric" optical thickness and measurements taken at Manua Loa observatory

Vermote, E., Saleous, N.E., Kaufman, Y.J. and Dutton, E., 1997. Data pre-processing: Stratospheric aerosol perturbing effect on the remote sensing of vegetation: Correction method for the composite NDVI after the Pinatubo eruption. Remote Sensing Reviews, 15(1-4), pp.7-21.

El Chichon and Pinatubo

Comparison of the Stratospheric AOT obtained from AVHRR with SAGE data for September 1982 (El Chichon eruption)

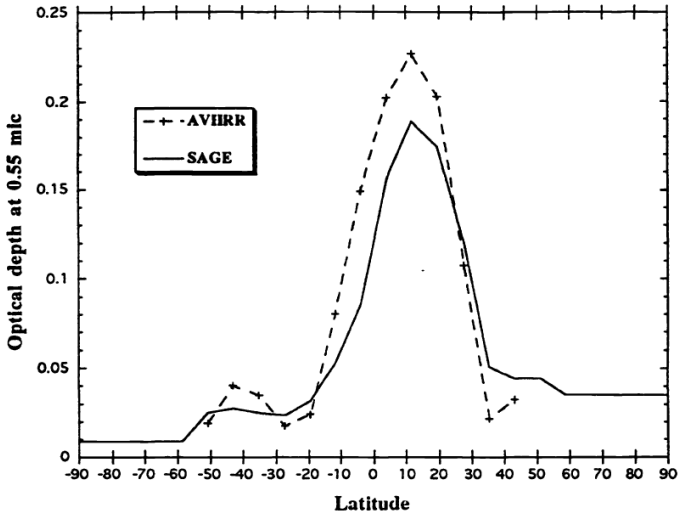

Figure 6: Latitudinal "stratospheric" profile observed after Mt. Pinatubo eruption.

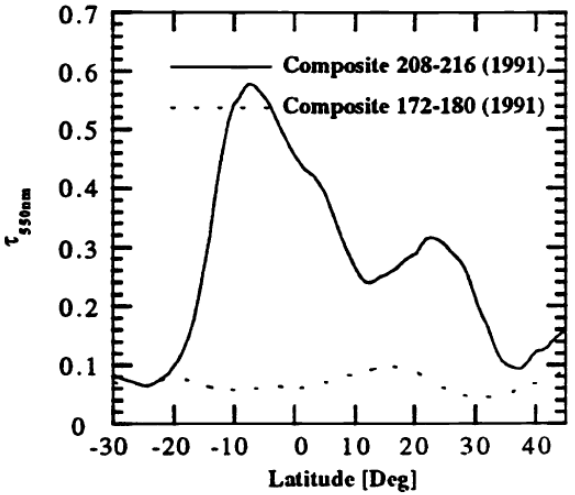

Eric F. Vermote, Nazmi El Saleous, "Stratospheric aerosol perturbing effect on the remote sensing of vegetation: operational method for the correction of AVHRR composite NDVI," Proc. SPIE 2311, Atmospheric Sensing and Modelling, (4 January 1995);

Generic Surface reflectance algorithm

The Surface reflectance algorithm relies on

- the use of very accurate (better than 1%) vector radiative transfer modeling of the coupled atmosphere-surface system
- the inversion of key atmospheric parameters (aerosol, water vapor)

Home page: http://modis-sr.ltdri.org

Generic flowchart for atmospheric correction

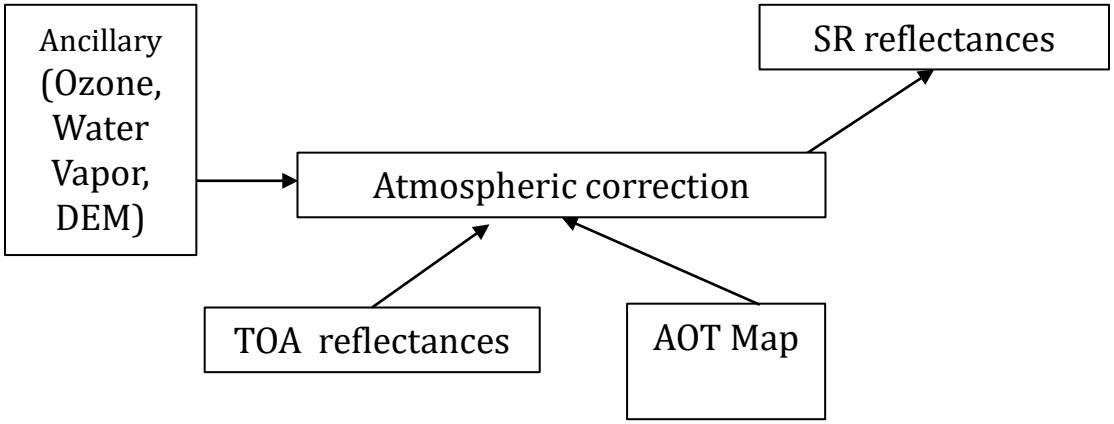

Generic Aerosol inversion

Reading **Inputs, LUT** and **Ancillary data**

ρ_{surf} determined (*) using ρ_{atm}, T_{atm} and S_{atm} **from LUT** assuming AOT, Aerosol model and knowing pressure, altitude, water vapor, ozone…

Aerosol Opt. Thick. and **Aerosol model** for each pixel

Using an assumed relationship between the blue surface reflectance (~450nm) and the red surface reflectance (~650nm) and fixing the aerosol model we are able to retrieve the **AOT.**

We loop the AOT until $(\rho_{surf}\ \text{blue} / \rho_{surf}\ \text{red})_{derived} = (\rho_{surf}\ \text{blue} / \rho_{surf}\ \text{red})_{assumed}$

The retrieved AOT is used to compute the surface reflectance at other wavelengths in the blue and SWIR to make a more robust inversion and refine the aerosol model. by minimizing the residual.

$$residual = \frac{\sum_{i=1}^{2}\left(\rho_{surf}^{i} - Ratio_{665}^{i} * \rho_{surf}^{665}\right)}{2}$$

Surface reflectance for each pixel and each band

Computation of **surface reflectances** for all channels

ρ_{surf} determined (*) using ρ_{atm}, T_{atm} and S_{atm} **from LUT** knowing AOT, Aerosol model, pressure, altitude, water vapor, ozone…

$$(*)\quad \rho_{surf} = \frac{Y}{1 + S_{atm}.Y} \quad \text{with} \quad Y = \frac{1}{T_{atm}.tg^{wv}}\left[\left(\frac{\rho_{TOA}}{tg^{O3}.tg^{others}} - \right) - \left(\rho_{atm} - \rho_{ray}\right).tg^{wv/2} - \rho_{ray}\right]$$

Methodology for evaluating the performance of surface reflectance

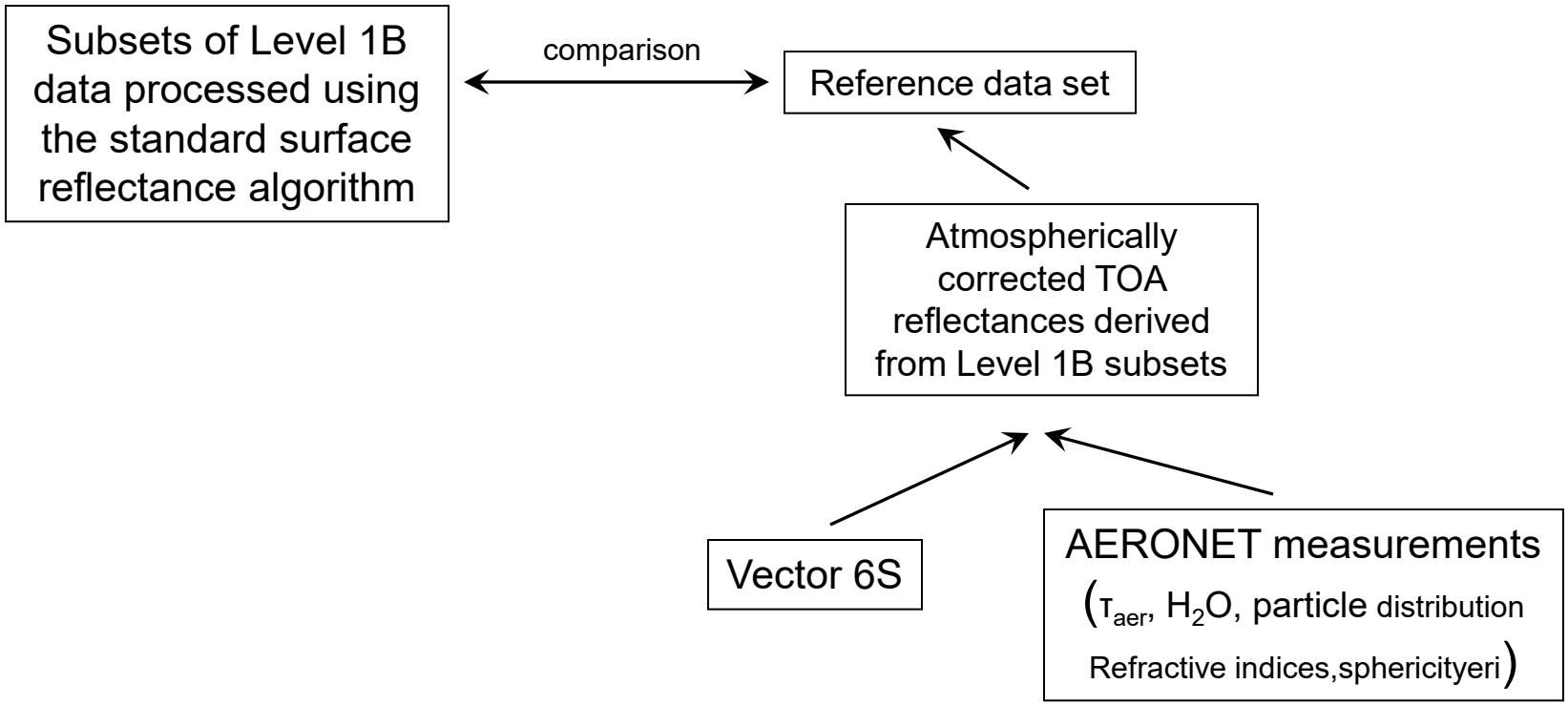

http://mod09val.ltdri.org/cgi-bin/mod09_c005_public_allsites_onecollection.cgi

quantitative assessment of performances (APU) for MODIS (Collection 5: Fixed ratio blue/red)

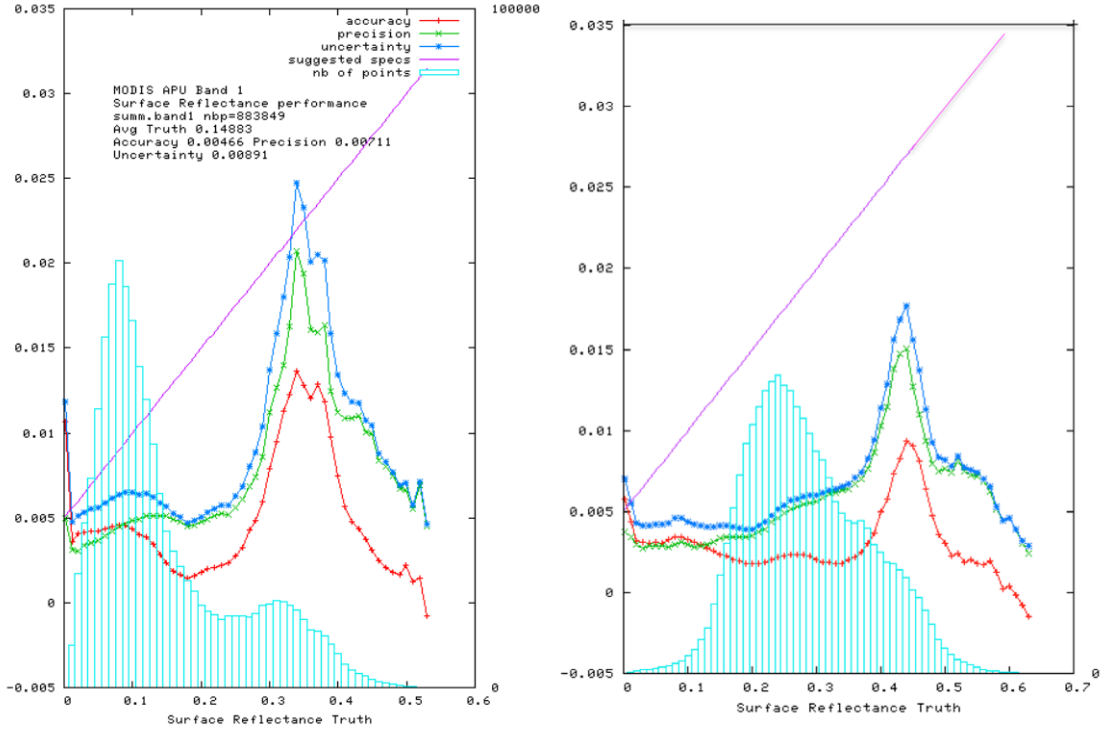

COLLECTION 5: accuracy or mean bias (red line), Precision or repeatability (green line) and Uncertainty or quadratic sum of Accuracy and Precision (blue line) of the surface reflectance in band 1 in the Red (top left), band 2 in the Near Infrared (top right also shown is the uncertainty specification (the line in magenta), that was derived from the theoretical error budget. Data collected from Terra over 200 AERONET sites from 2000 to 2009.

Improving the aerosol retrieval in collection 6 reflected in APU metrics

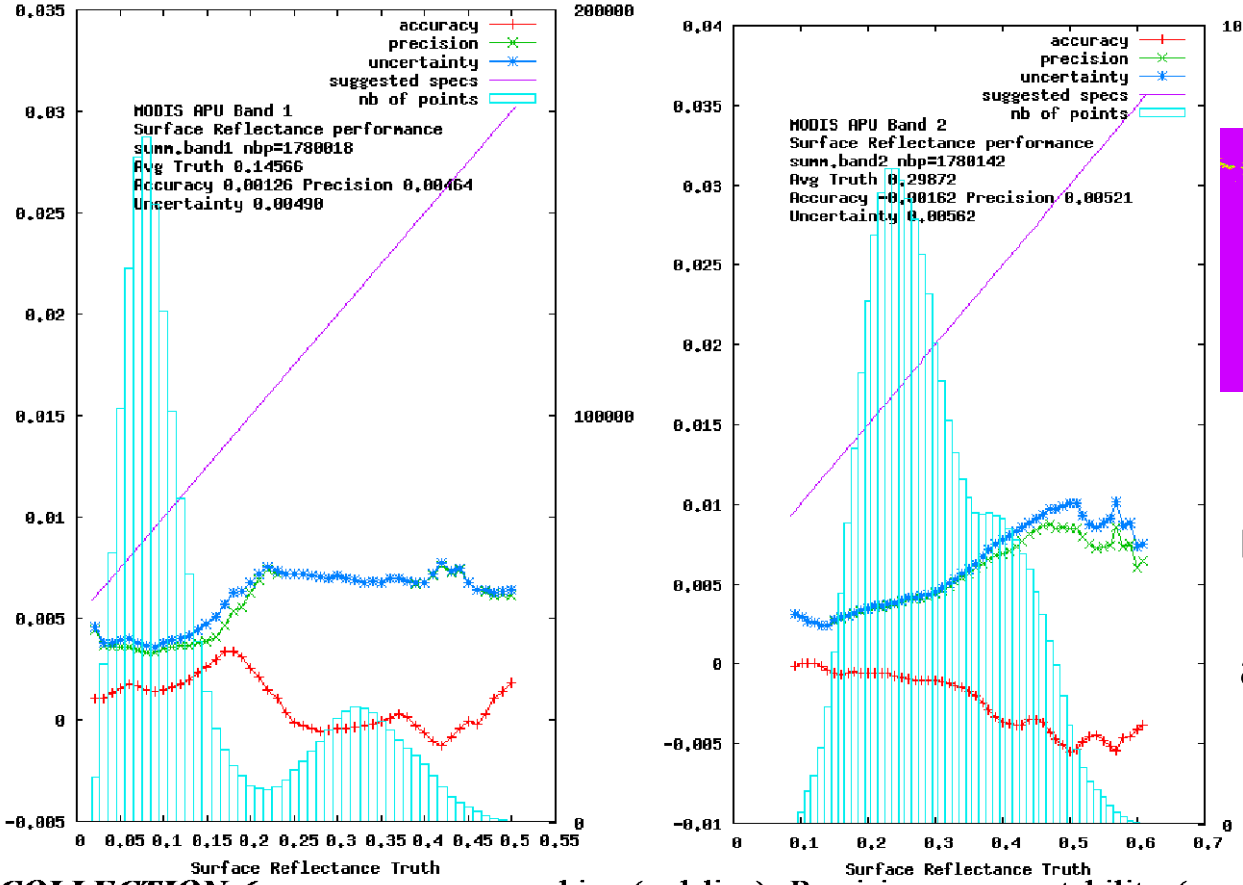

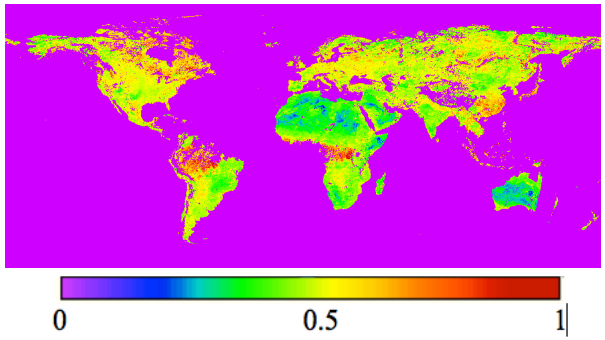

ratio blue/red derived using MODIS top of the atmosphere corrected with MISR aerosol optical depth

COLLECTION 6: accuracy or mean bias (red line), Precision or repeatability (green line) and Uncertainty or quadratic sum of Accuracy and Precision (blue line) of the surface reflectance in band 1 in the Red (top left), band 2 in the Near Infrared (top right also shown is the uncertainty specification (the line in magenta), that was derived from the theoretical error budget. Data collected from Terra over 200 AERONET sites for the whole Terra mission.

Aerosol retrieval also shows improvement

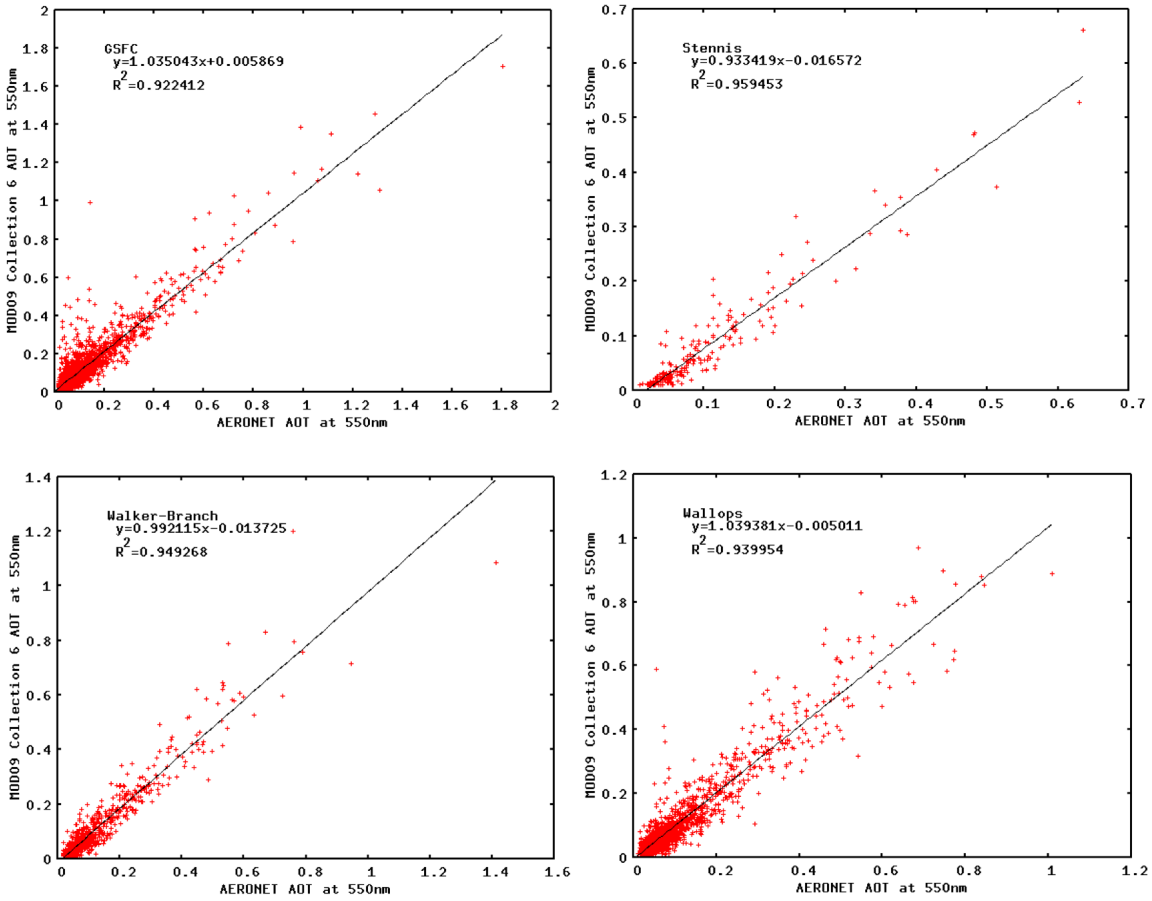

Scatterplot of the MOD09 AOT at 550nm versus the AERONET measured AOT at 550nm for East Coast sites selection: GSFC (top left), Stennis (top right), Walker Branch (bottom left) and Wallops (bottom right).

Aerosol retrieval also shows improvement

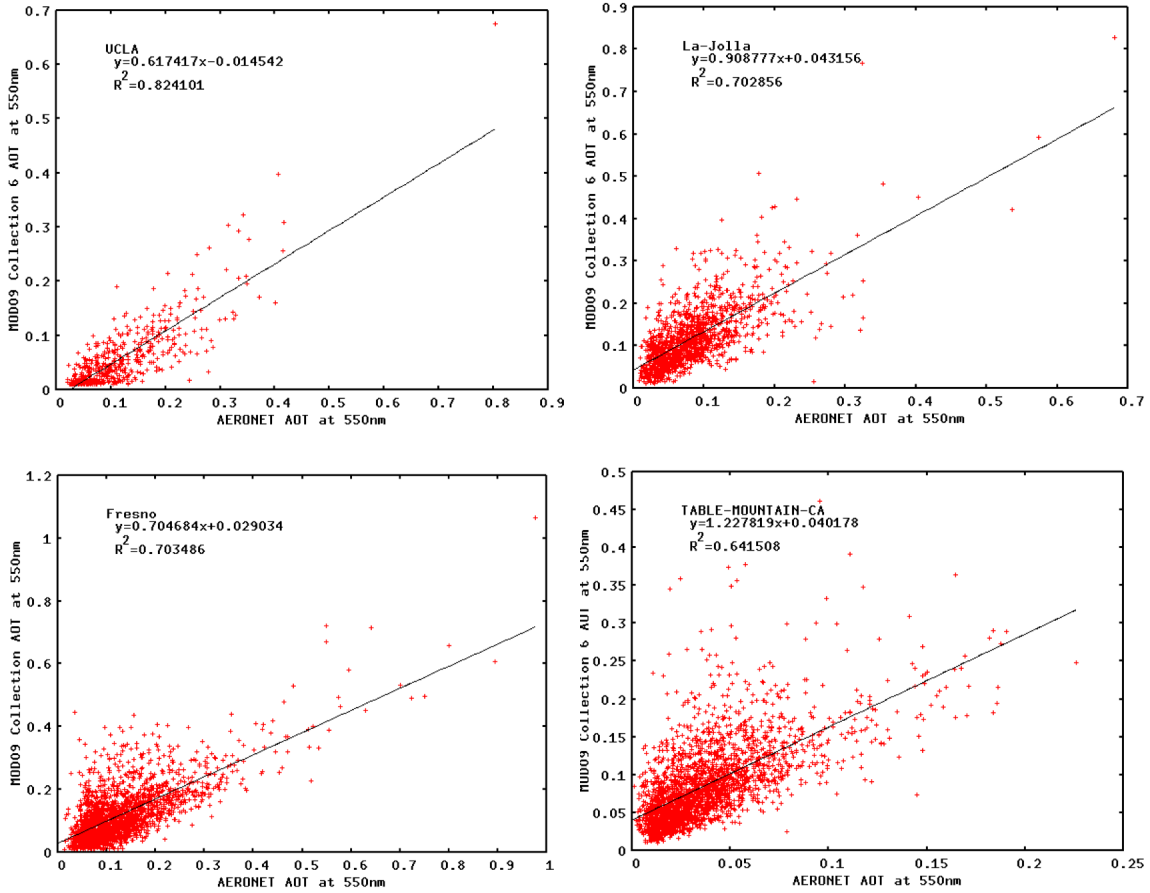

Scatterplot of the MOD09 AOT at 550nm versus the AERONET measured AOT at 550nm for the West Coast sites selection: UCLA (top left), La Jolla (top right), and Fresno (bottom left) and Table Mountain (bottom right).

Aerosol retrieval also shows improvement

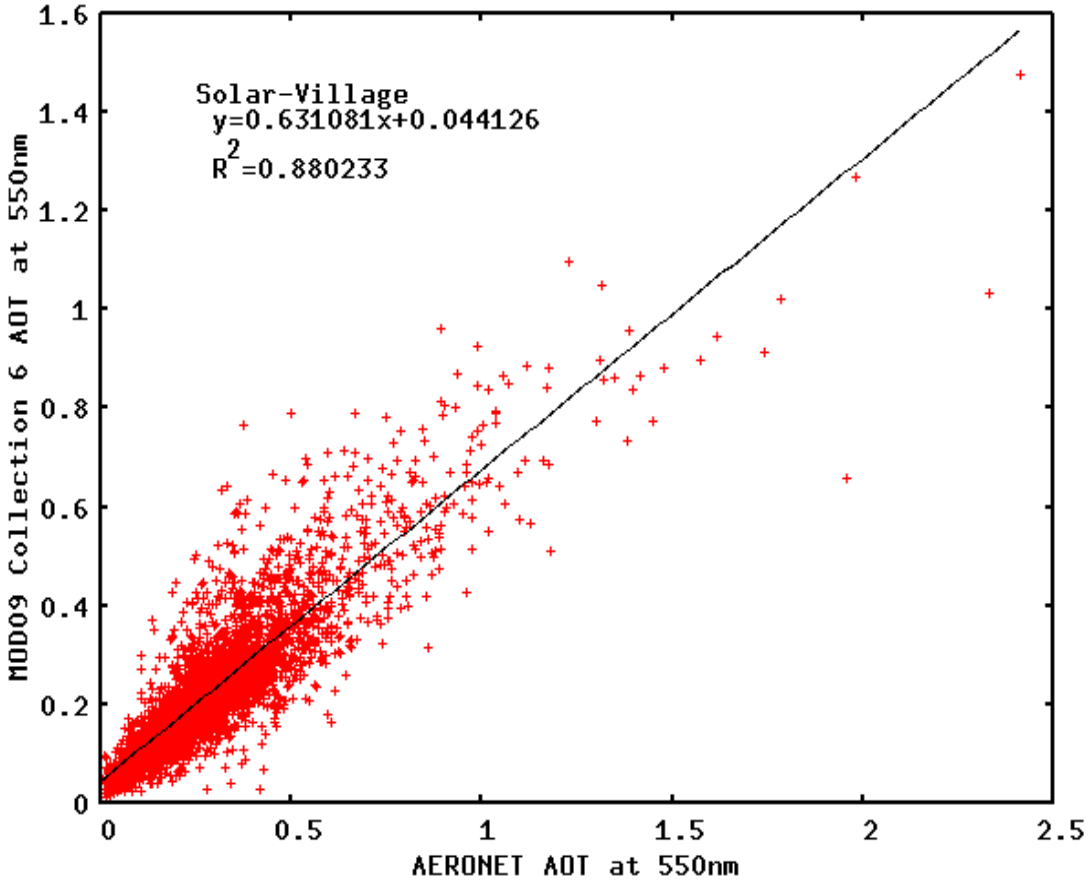

Scatterplot of the MOD09 AOT at 550nm versus the AERONET measured AOT at 550nm for for a very bright site in Saudi Arabia (Solar Village)

Landsat8/OLI and Sentinel 2/MSI Surface Reflectance is largely based on MODIS C6 (LaSRC)

Algorithm reference for L8: Vermote E., Justice C., Claverie M., Franch B., (2016) “Preliminary analysis of the performance of the Landsat 8/OLI land surface reflectance product", Remote Sensing of Environment, 185,46-56.

The MODIS **Collection 6 AC algorithm** relies on

- the use of very accurate (better than 1%) vector radiative transfer modeling of the coupled atmosphere-surface system (6S)
- the inversion of key atmospheric parameters
  - ***Aerosols are retrieved from Landsat8/Sentinel 2 images***
  - ***Water vapor and ozone from daily MODIS product.***

Home page: http://modis-sr.ltdri.org

Evaluation of the performance of Landsat8

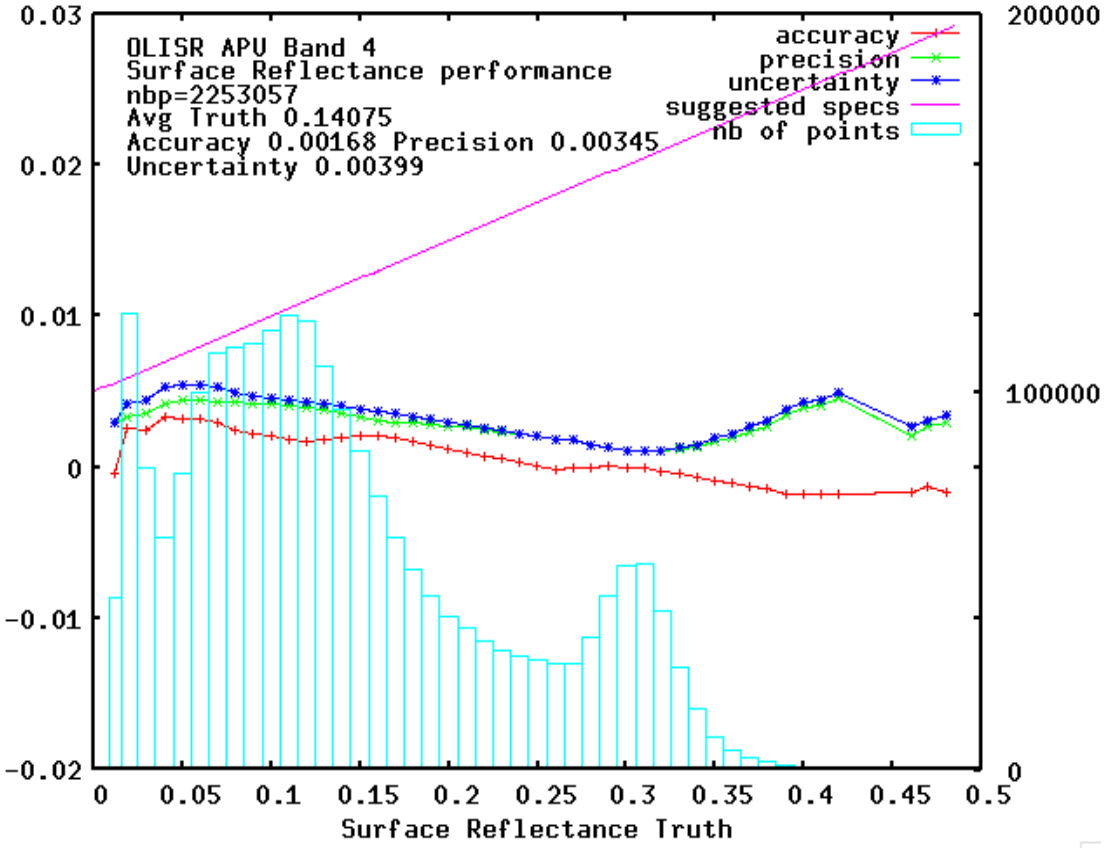

The “preliminary” analysis of OLI SR performance in the red band over AERONET is very similar to MODIS Collection 6

This is confirmed by comparison with MODIS

OLI Band	TM LEDAPS (Claverie et al., 2015)			ETM+ LEDAPS (Claverie et al., 2015)			OLI (Vermote et al., 2016)		
	A	P	**U**	A	P	**U**	A	P	**U**
2	7	9	**11**	9	7	**12**	2	6	**6**
3	1	9	**9**	6	9	**11**	3	6	**7**
4	9	10	**14**	1	9	**9**	1	6	**6**
5	5	17	**17**	3	14	**15**	2	12	**12**
7	1	14	**14**	5	15	**16**	9	11	**14**

OLI surface reflectance APU scores expressed in 10^{-3} reflectance (compared to TM and ETM+ surface reflectance APU by Claverie et al. (2015) using Aqua MODIS BRDF and spectrally adjusted surface reflectance CMG product as reference, the OLI surface reflectance was aggregated over the CMG. Band number corresponds to OLI band number designation and equivalent TM/ETM+ bands were reported.

LaSRC AOT Results on ACIX-II

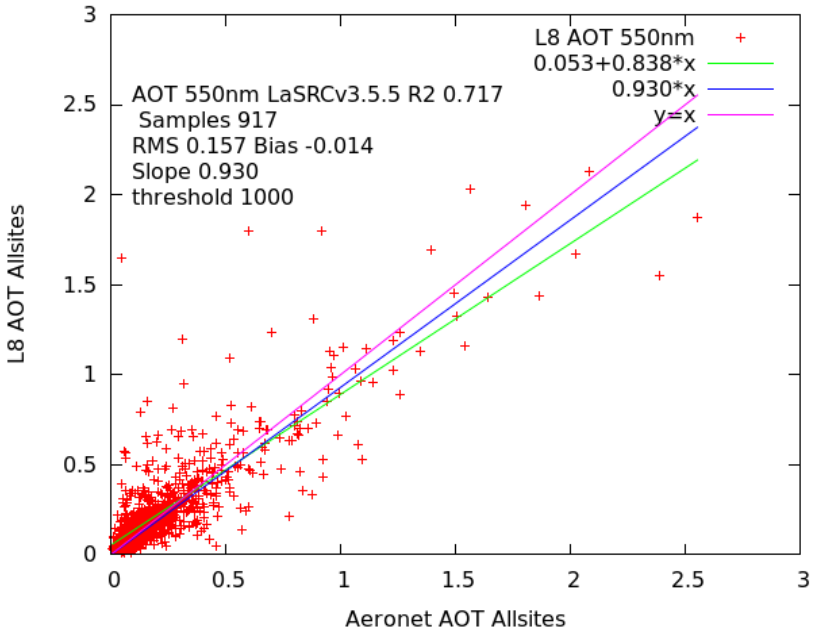

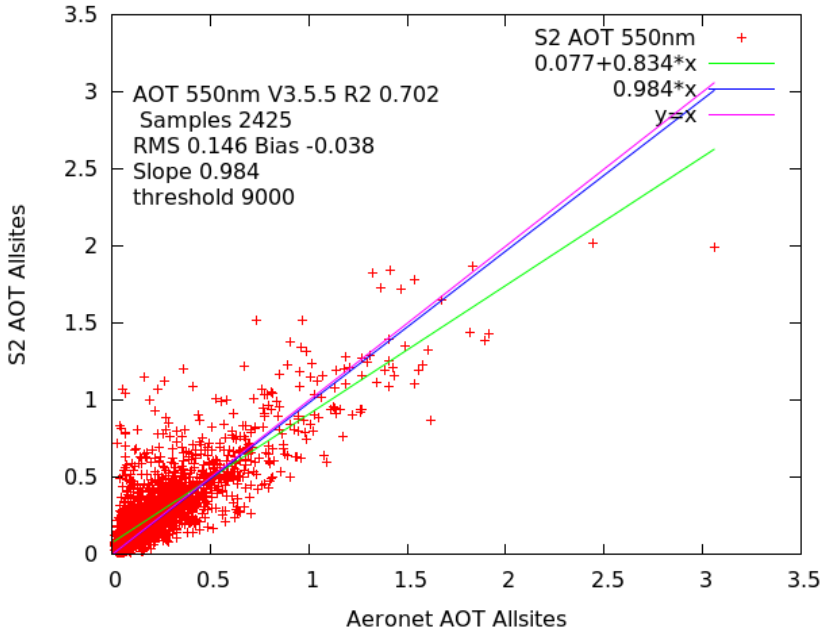

LaSRC APU results on ACIX-II

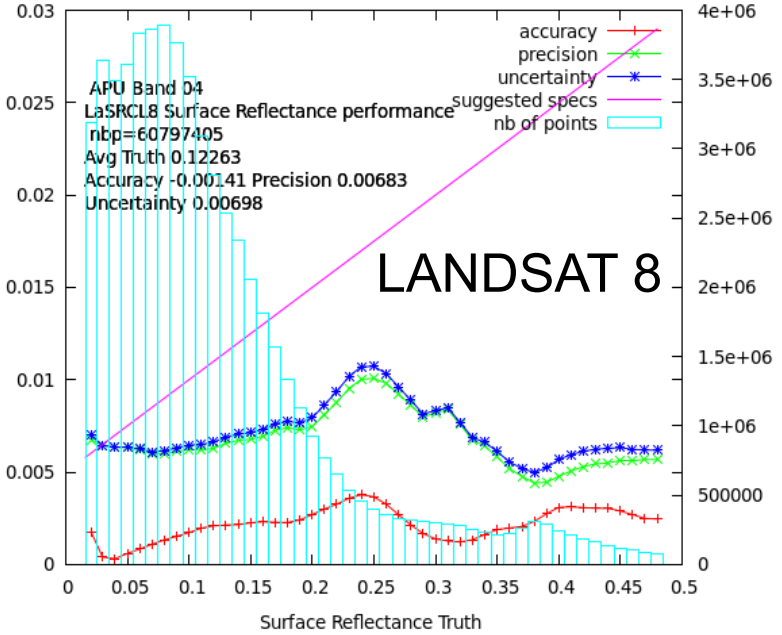

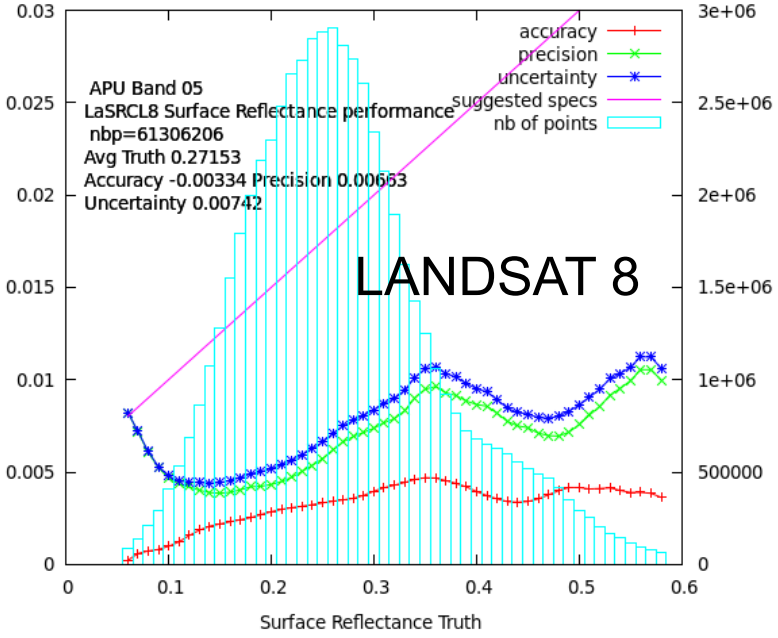

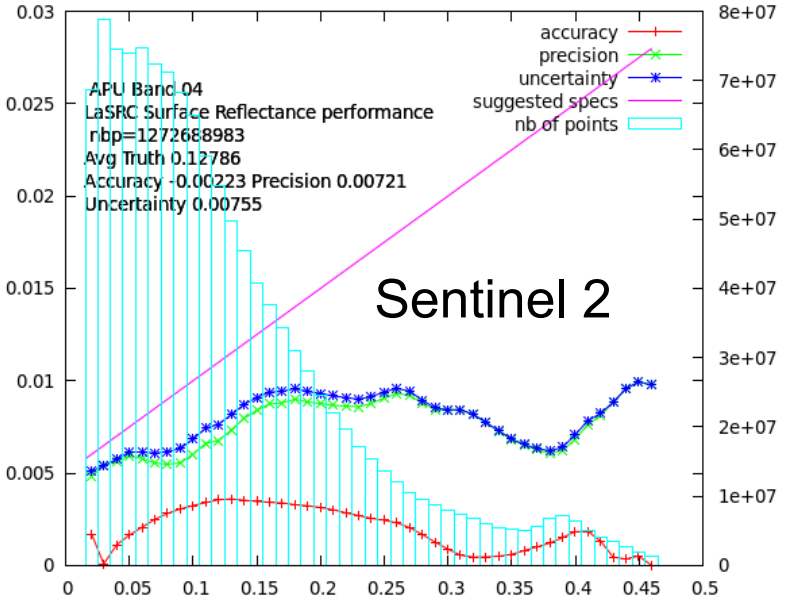

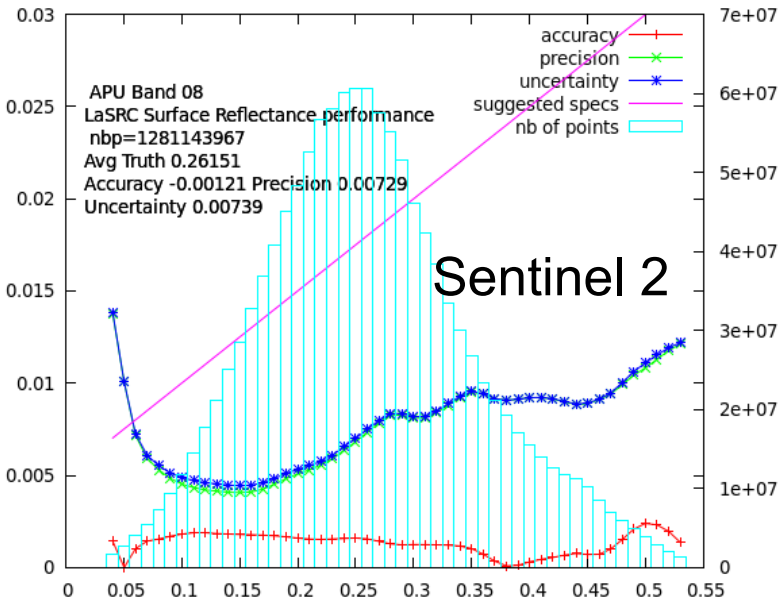

Performances on AOD retrieval over urban environment

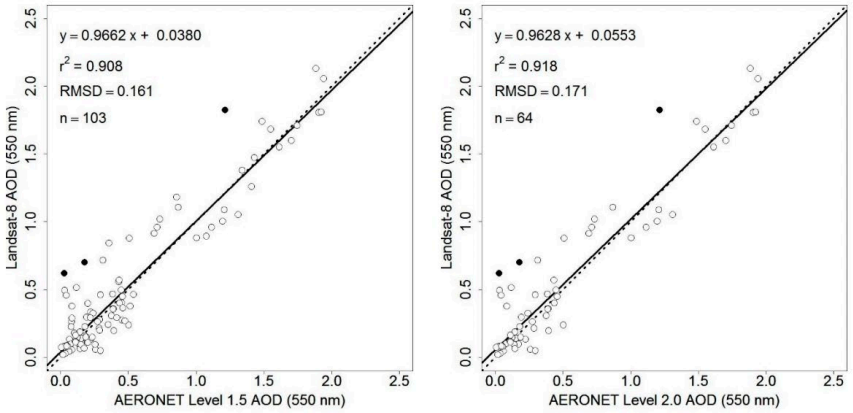

Figure 3. Scatterplots of the Landsat-8 AOD against the contemporaneous AERONET Level 1.5 (**left**) and Level 2.0 (**right**) AOD data over the urban AERONET sites for 2016. The three filled circles are outliers due to Landsat-8 cloud detection omission errors and are not used in statistics analysis. The solid lines show ordinary least square regression lines. The dotted lines are 1:1 lines superimposed for reference.

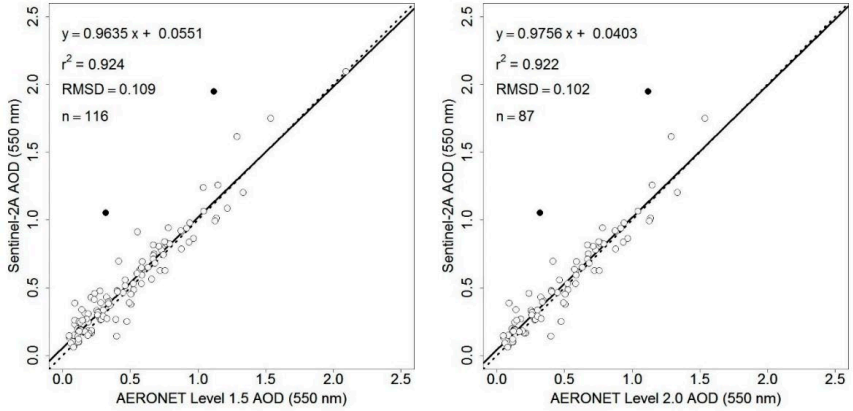

Figure 4. Scatterplots of the Sentinel-2A AOD against the contemporaneous AERONET Level 1.5 (**left**) and Level 2.0 (**right**) AOD data over the urban AERONET sites for 2016. The two filled circles are outliers due to Sentinel-2A cloud detection omission errors and are not used in statistics analysis. The solid lines show ordinary least square regression lines. The dotted lines are 1:1 lines superimposed for reference.

Li, Z., Roy, D. P., Zhang, H. K., Vermote, E. F., & Huang, H. (2019). Evaluation of Landsat-8 and Sentinel-2A aerosol optical depth retrievals across Chinese cities and implications for medium spatial resolution urban aerosol monitoring. *Remote sensing*, *11*(2), 122.

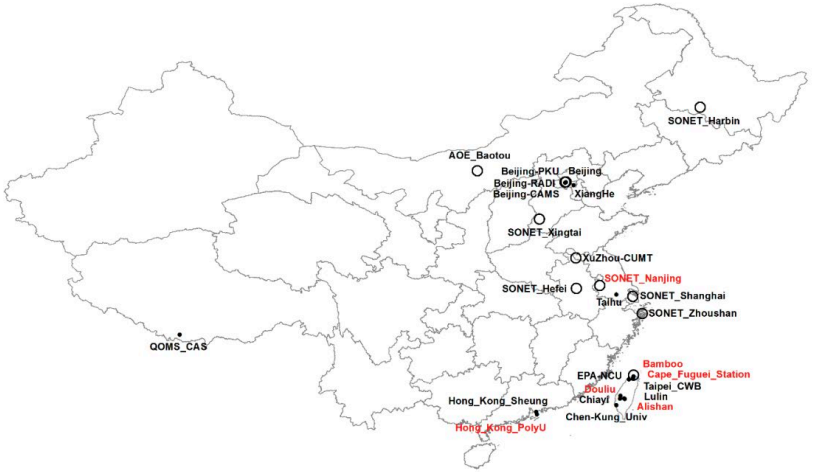

Ground Validation using episodic ground measurements over uniform/stable/arid sites

Ratio of L9 and L8 Surface Reflectance Products					
Band	**Guymon (ECCOE)**	**Coconino (ECCOE)**	**Ivanpah Playa (UArizona)**	**Seven Persons (U of Lethbridge)**	**Wilcannia (GA)**
Coastal/ Aerosol	0.995	0.999	0.97	0.996	1.005
Blue	0.980	1.023	0.99	0.974	1.001
Green	0.987	1.015	1.01	0.991	1.002
Red	0.991	1.019	1.00	0.986	0.998
NIR	0.999	1.014	0.98	0.979	1.001
SWIR1	0.995	1.011	1.02	0.994	1.007
SWIR2	0.989	1.026	1.03	0.982	0.994

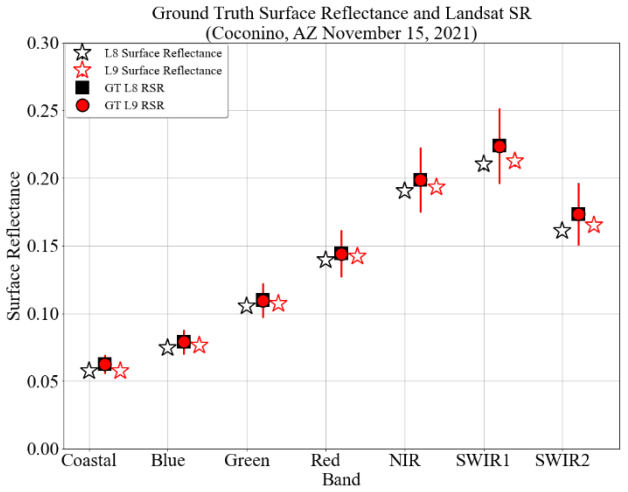

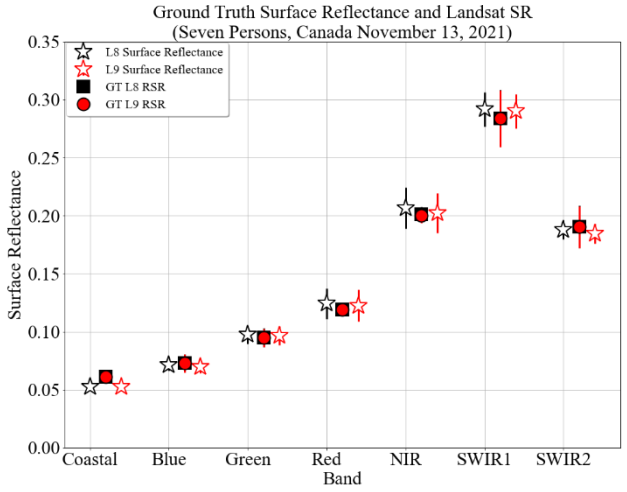

Time series analysis

GSFC-BELTSVILLE Site 1920 meters x 1920 meters

August 2019 (S2B) | August 2015 (S2A) | Google Earth (Oct 2020,Sept 2021)

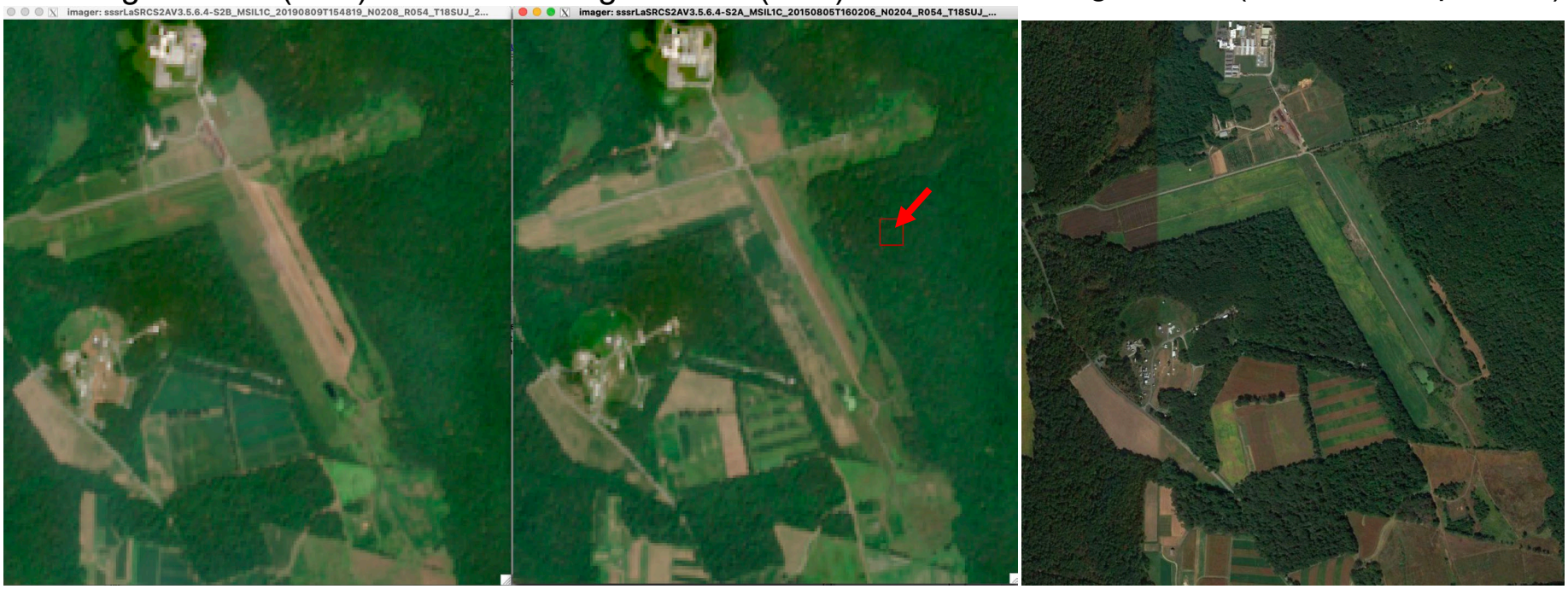

$$Noise = \sqrt{\frac{\sum_{i=1}^{n-2}\left(\rho_{i+1} - \frac{\rho_{i+2}-\rho_i}{d_{i+2}-d_i}(d_{i+1}-d_i) - \rho_i\right)^2}{n-2}}$$

Original formula Vermote et al. 2019 (with threshold 20 days)

Time Series and noise with threshold at 60 days

Surface reflectance LaSRC S2A,B

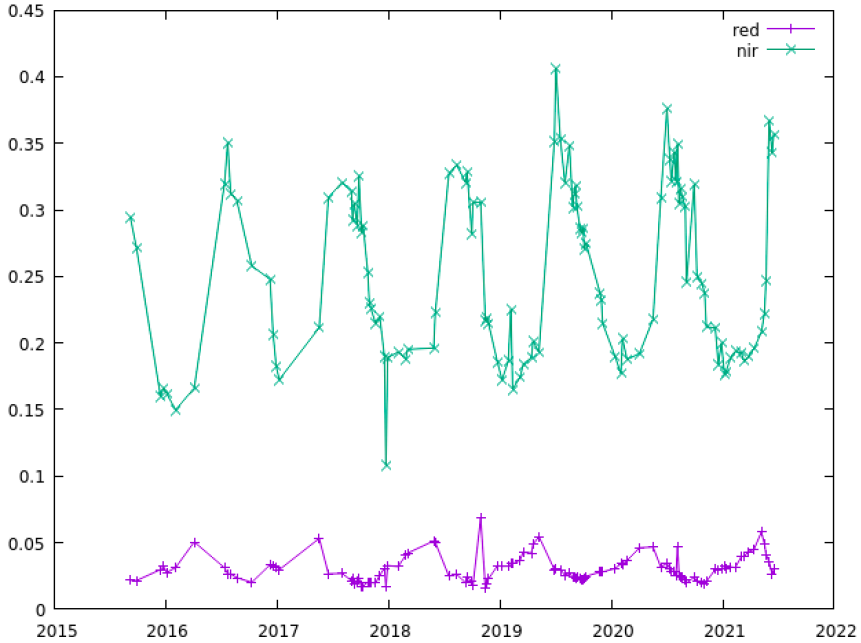

band	Avg	Std	CV Std/Avg	NB
red	0.030	0.010	0.326	116
nir	0.252	0.064	0.255	116

band	Noise	Noise (95%)	NB
red	0.003	0.003	94/89
nir	0.021	0.022	94/89

Surface reflectance LaSRC S2A,B no QA applied

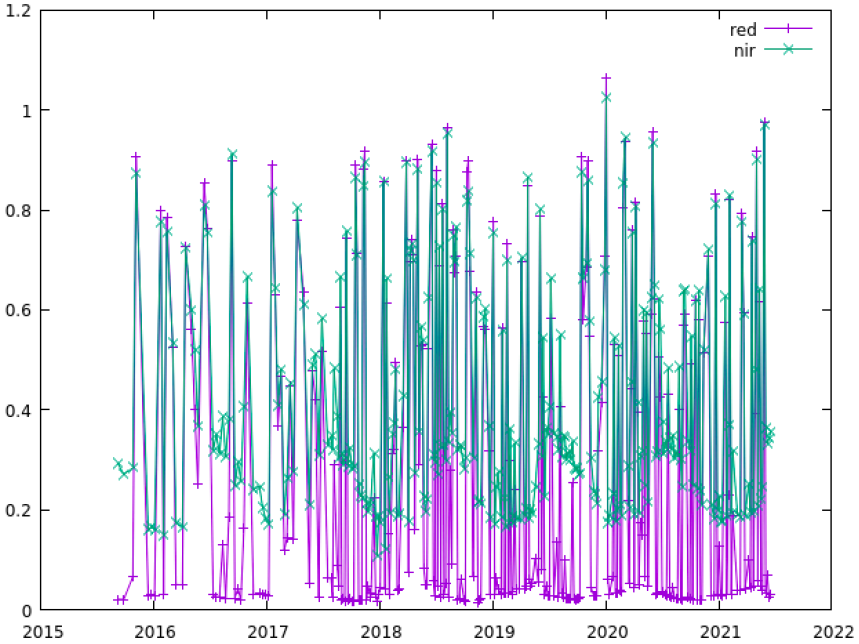

band	Avg	Std	CV Std/Avg	NB
red	0.277	0.314	1.134	296
nir	0.415	0.227	0.547	296

band	Noise	Noise (95%)	NB
red	0.332	0.340	294/279
nir	0.239	0.245	294/279

Time Series and metrics (threshold at 60 days)

Surface reflectance LaSRC (QA Next generation experimental applied)

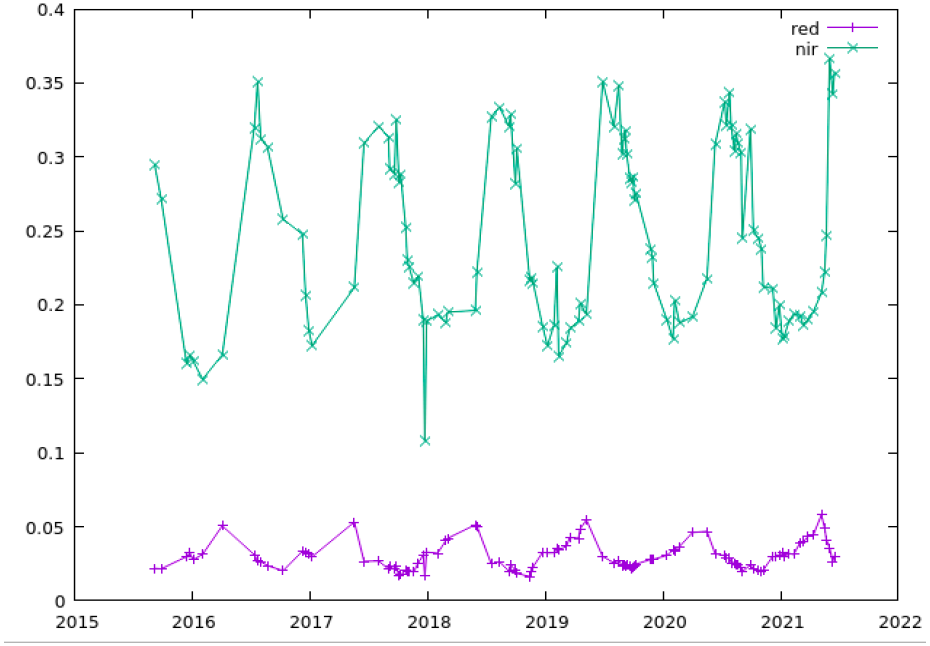

band	Avg	Std	CV	NB
red	0.030	0.009	0.310	110
nir	0.247	0. 061	0.248	116

band	Noise	Noise (95%)	NB
red	0.002	0.002	87/82
nir	0.019	0.019	87/82

Combining with Landsat 8

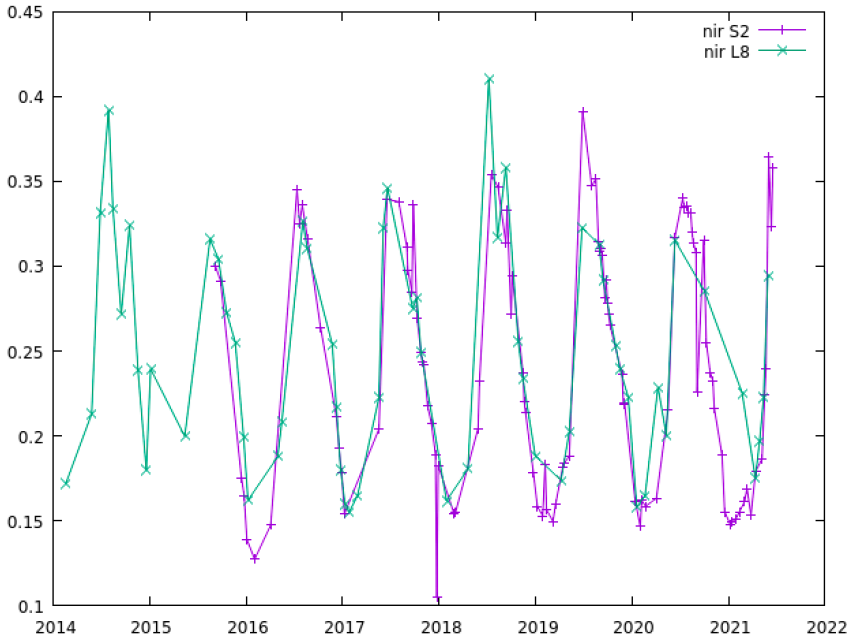

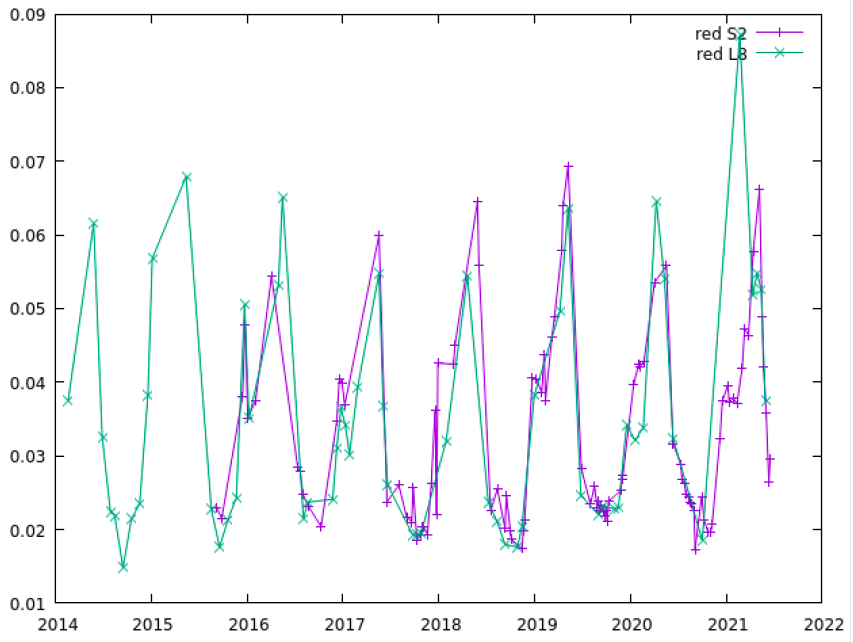

S2 (3x3)

band	Noise	Rnoise %	NB
red	0.0029	8.9	83
nir	0.0171	7.1	83

L8

band	Noise	Rnoise %	NB
red	0.0038	10.8	13
nir	0.0222	9.0	13

S2+L8

band	Noise	Rnoise %	NB
red	0.0036	10.7	146
nir	0.0201	8.3	146

RNoise = 100*Noise/average

Ground Validation using CAMSIS

CAMSIS system

CAMSIS is installed at a height of 123m on a TV tower (WLEF) near Park Falls, WI at the Chequamegon National Forest

CAMSIS Data processing

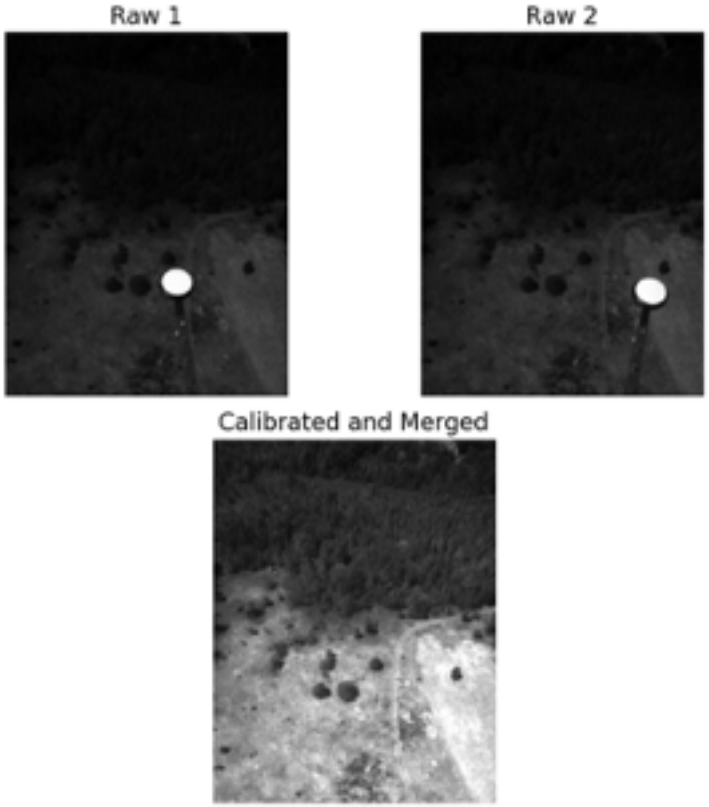

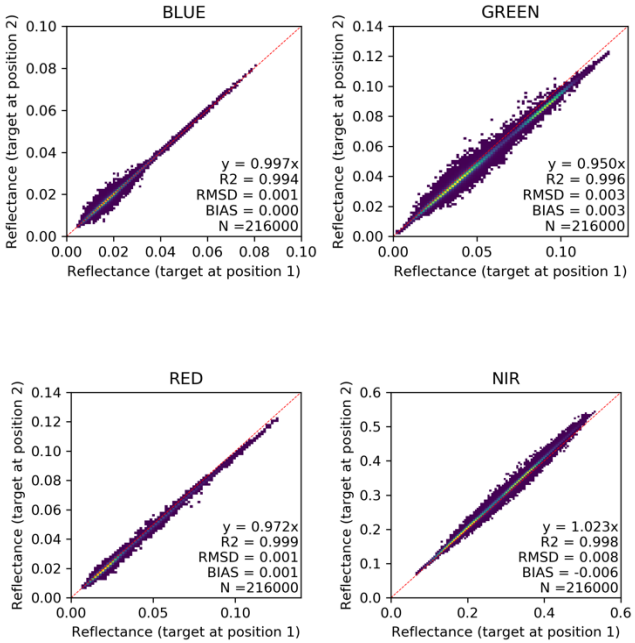

CAMSIS Data processing

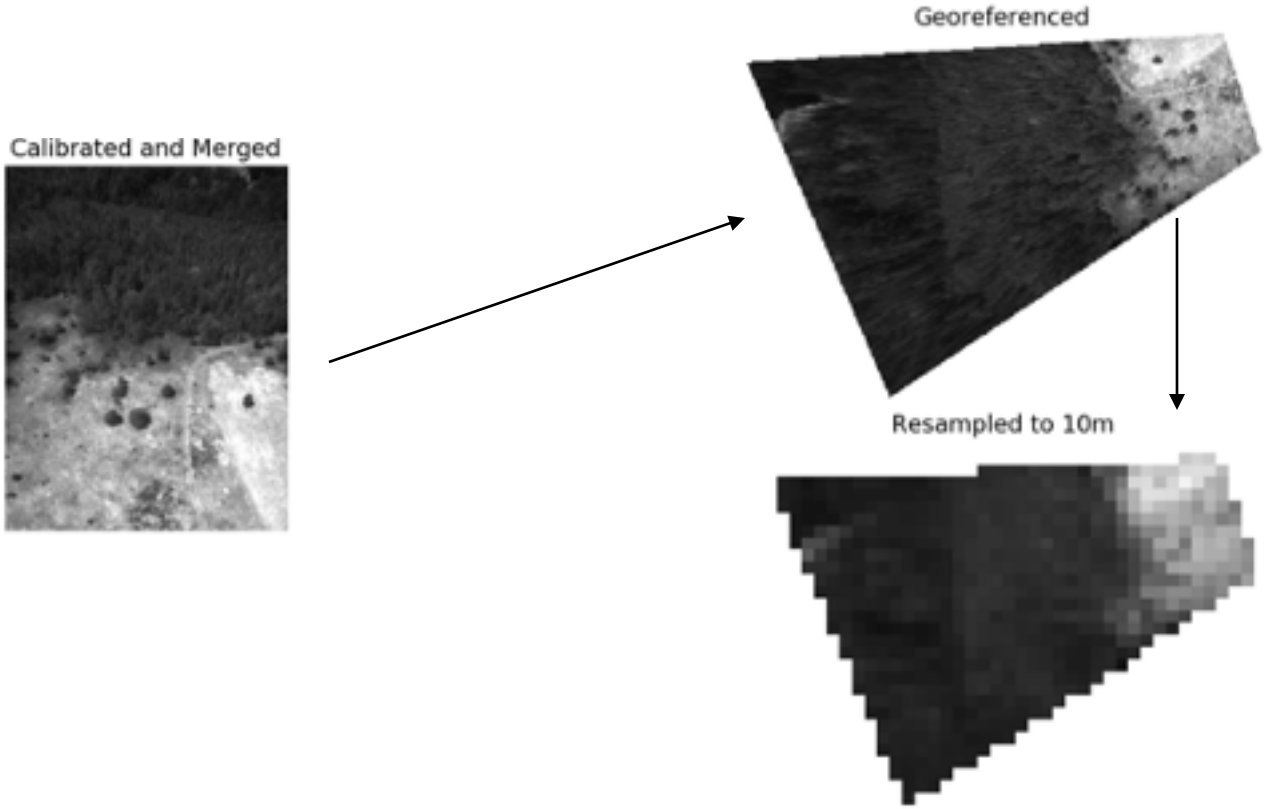

First results from CAMSIS on Sentinel 2

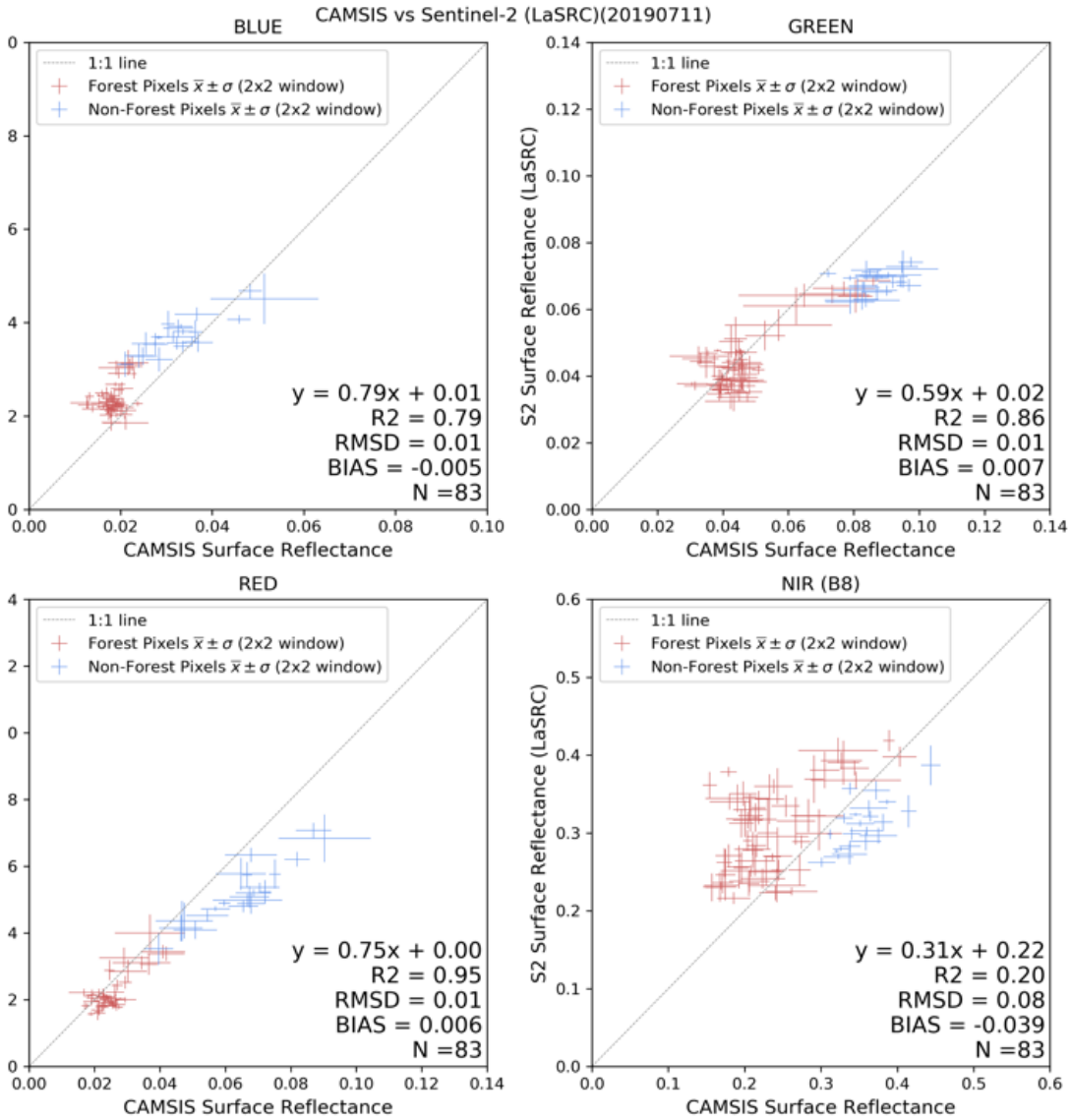

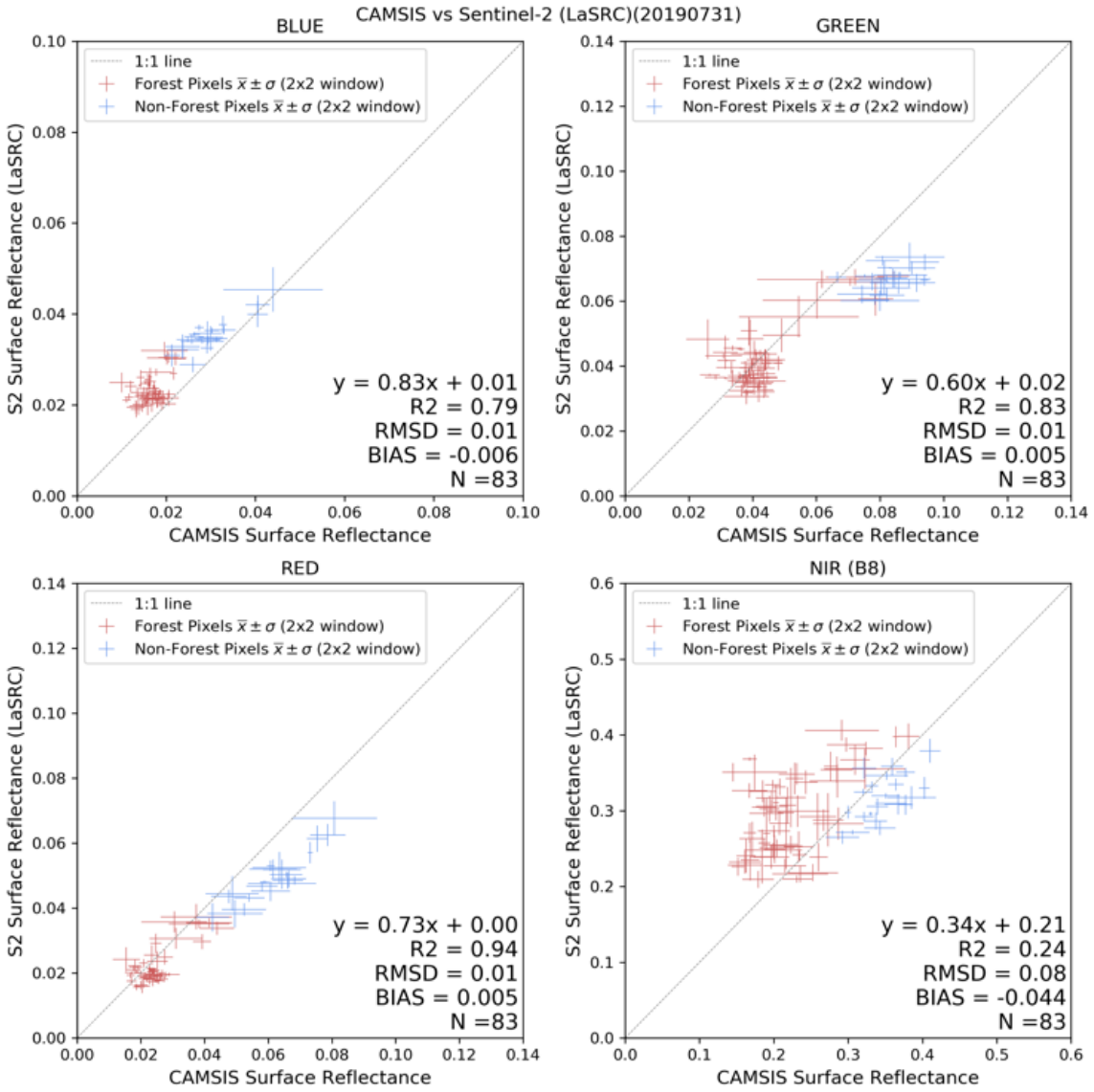
CAMSIS vs Sentinel-2 (LaSRC)(20190731)
BLUE
1:1 line
Forest Pixels $\bar{x} \pm \sigma$ (2x2 window)
Non-Forest Pixels $\bar{x} \pm \sigma$ (2x2 window)
y = 0.83x + 0.01
R2 = 0.79
RMSD = 0.01
BIAS = -0.006
N =83
GREEN
y = 0.60x + 0.02
R2 = 0.83
RMSD = 0.01
BIAS = 0.005
N =83
RED
y = 0.73x + 0.00
R2 = 0.94
RMSD = 0.01
BIAS = 0.005
N =83
NIR (B8)
y = 0.34x + 0.21
R2 = 0.24
RMSD = 0.08
BIAS = -0.044
N =83
S2 Surface Reflectance (LaSRC)
CAMSIS Surface Reflectance

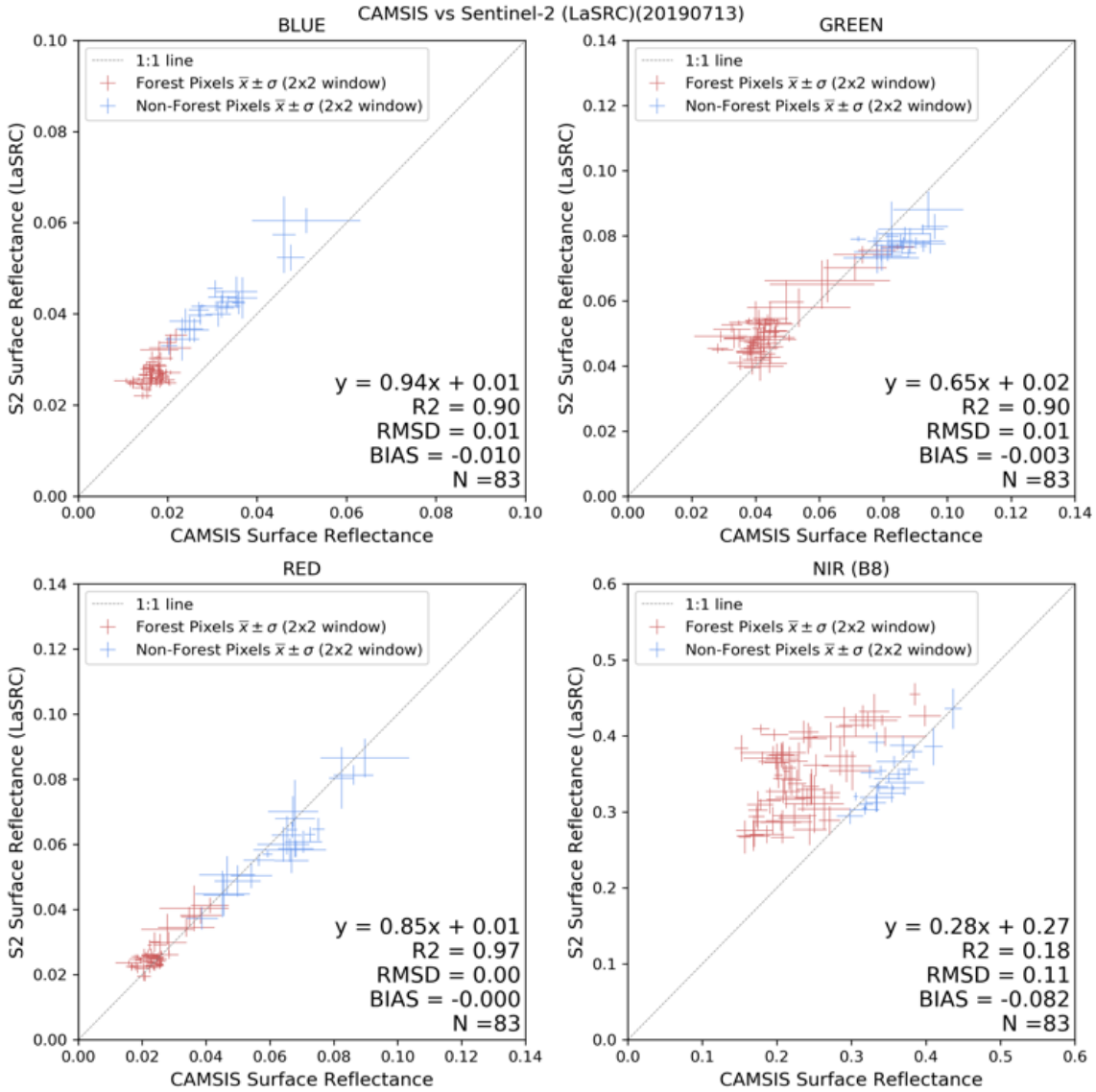
CAMSIS vs Sentinel-2 (LaSRC)(20190713)
BLUE
1:1 line
Forest Pixels $\bar{x} \pm \sigma$ (2x2 window)
Non-Forest Pixels $\bar{x} \pm \sigma$ (2x2 window)
y = 0.94x + 0.01
R2 = 0.90
RMSD = 0.01
BIAS = -0.010
N =83
GREEN
y = 0.65x + 0.02
R2 = 0.90
RMSD = 0.01
BIAS = -0.003
N =83
RED
y = 0.85x + 0.01
R2 = 0.97
RMSD = 0.00
BIAS = -0.000
N =83
NIR (B8)
y = 0.28x + 0.27
R2 = 0.18
RMSD = 0.11
BIAS = -0.082
N =83
S2 Surface Reflectance (LaSRC)
CAMSIS Surface Reflectance

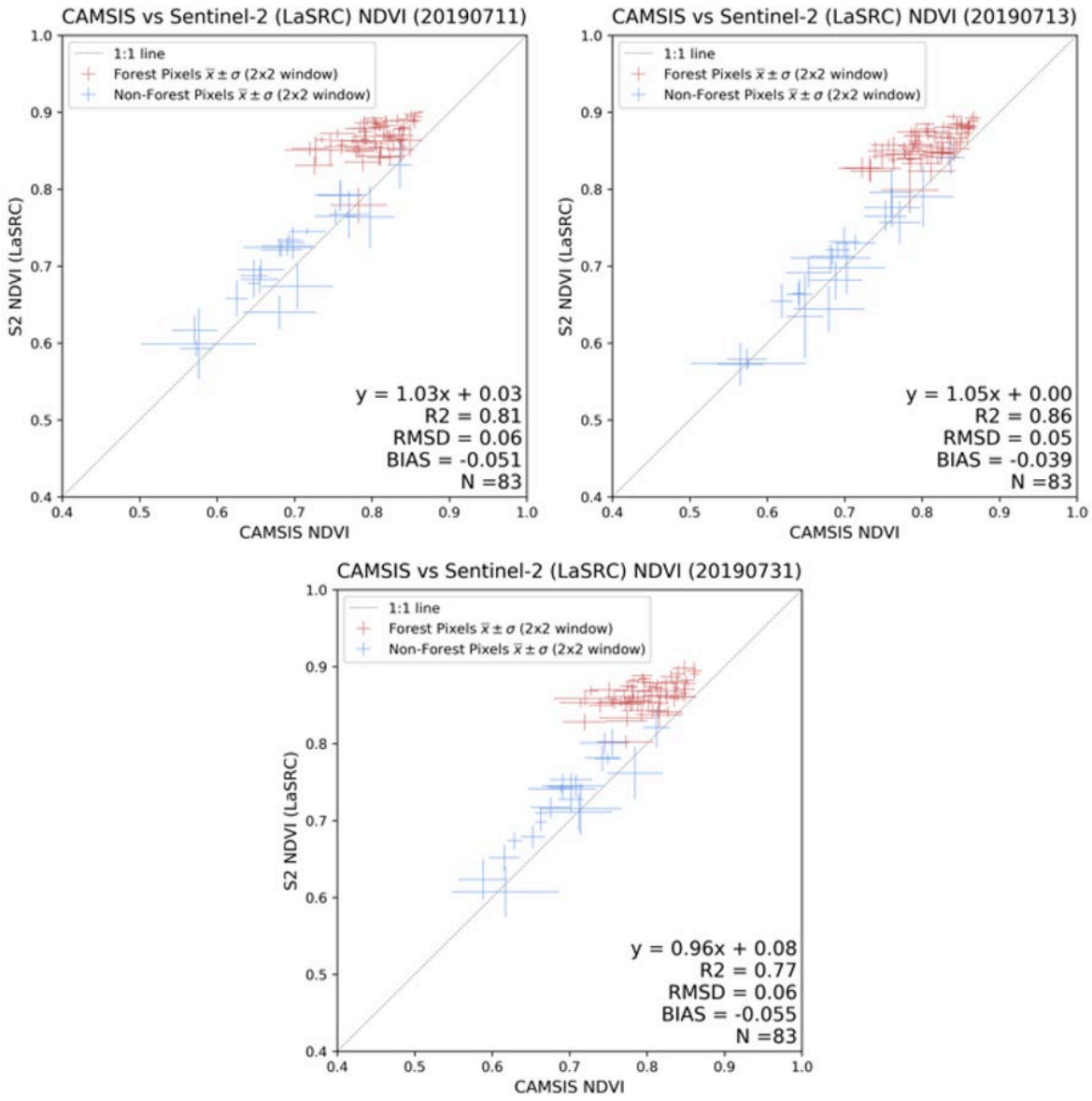
CAMSIS vs Sentinel-2 (LaSRC) NDVI (20190711)
1:1 line
Forest Pixels $\bar{x} \pm \sigma$ (2x2 window)
Non-Forest Pixels $\bar{x} \pm \sigma$ (2x2 window)
y = 1.03x + 0.03
R2 = 0.81
RMSD = 0.06
BIAS = -0.051
N =83
S2 NDVI (LaSRC)
CAMSIS NDVI
CAMSIS vs Sentinel-2 (LaSRC) NDVI (20190713)
1:1 line
Forest Pixels $\bar{x} \pm \sigma$ (2x2 window)
Non-Forest Pixels $\bar{x} \pm \sigma$ (2x2 window)
y = 1.05x + 0.00
R2 = 0.86
RMSD = 0.05
BIAS = -0.039
N =83
S2 NDVI (LaSRC)
CAMSIS NDVI
CAMSIS vs Sentinel-2 (LaSRC) NDVI (20190731)
1:1 line
Forest Pixels $\bar{x} \pm \sigma$ (2x2 window)
Non-Forest Pixels $\bar{x} \pm \sigma$ (2x2 window)
y = 0.96x + 0.08
R2 = 0.77
RMSD = 0.06
BIAS = -0.055
N =83
S2 NDVI (LaSRC)
CAMSIS NDVI

Cloud validation: SkyCam

- Ground-based skycam
  - For objective validation of satellite-derived cloud masks
  - Proof of concept: manual iphone with fisheye lens over NASA GSFC
  - Current version: automatic, enabling replication over multiple sites
  - Part of validation dataset within CEOS CMIX-1 (Cloud Masking Inter-comparison Exercise)

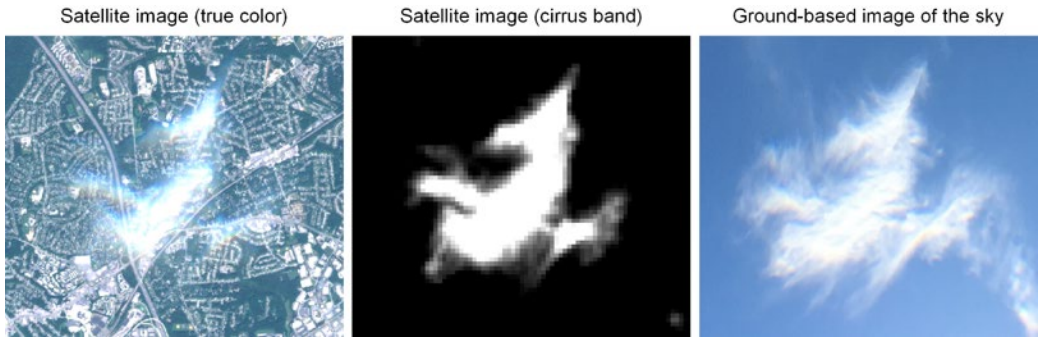

International Journal of Applied Earth Observations and Geoinformation 95 (2021) 102253

Contents lists available at ScienceDirect

International Journal of Applied Earth Observations and Geoinformation

journal homepage: www.elsevier.com/locate/jag

An experimental sky-image-derived cloud validation dataset for Sentinel-2 and Landsat 8 satellites over NASA GSFC

Sergii Skakun [a,b,c,*], Eric F. Vermote [c], Andres Eduardo Santamaria Artigas [a,c], William H. Rountree [a,c], Jean-Claude Roger [a,c]

[a] Department of Geographical Sciences, University of Maryland, College Park, MD 20742, USA
[b] College of Information Studies (iSchool), University of Maryland, College Park, MD 20742, USA
[c] NASA Goddard Space Flight Center Code 619, 8800 Greenbelt Road, Greenbelt, MD 20771, USA

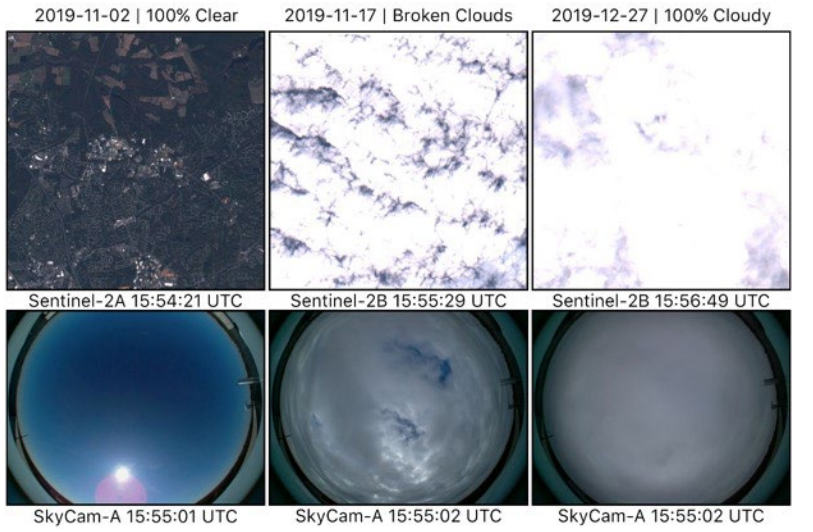

SkyCam system @ NASA/GSFC

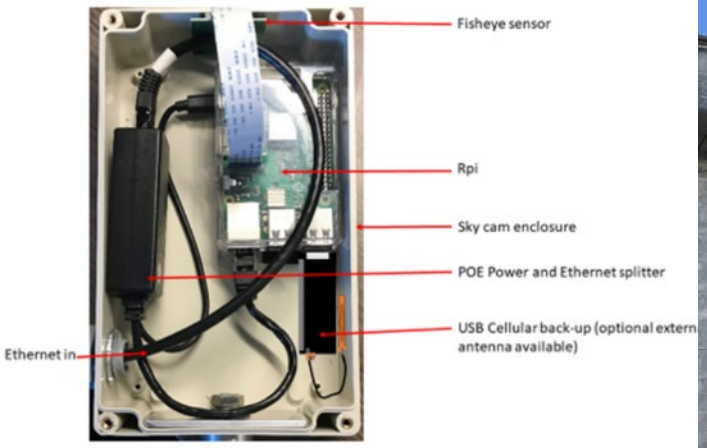

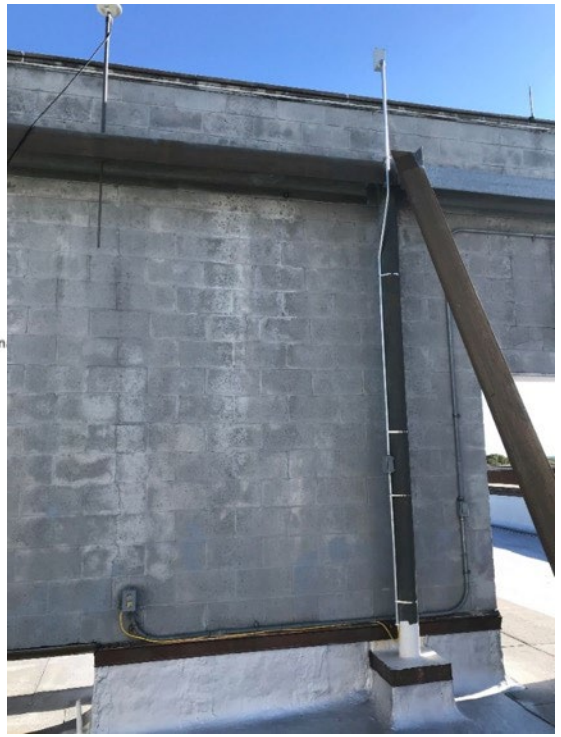

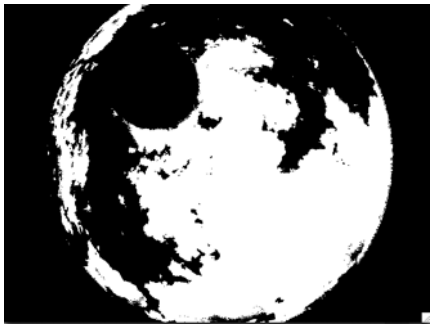

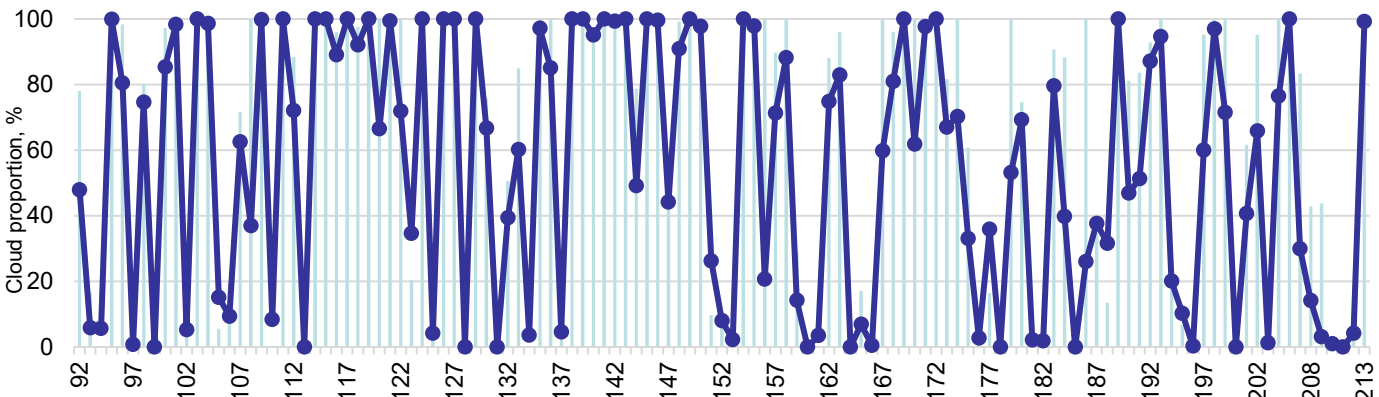

Skycam current and *near future* deployment (dual camera)

GSFC, Greenbelt, Maryland, USA
Sapienza University, Rome, Italy
Valencia University, Valencia, Spain
Sao Paulo University, Sao Paulo, Brazil
Princess Elisabeth Station, Antarctica

WLEF, Park Falls, Wisconsin, USA
ATTO Brazil

Conclusions

- Surface reflectance (SR) algorithm is mature and pathway toward validation and automated QA is clearly identified.
- Algorithm is generic and tied to documented validated radiative transfer code so the accuracy is traceable enabling error budget.
- The use of BRDF correction enables easy cross-comparison of different sensors (MODIS,VIIRS,AVHRR, Landsat, Sentinel 2 ,Sentinel 3…).
- We are proposing a complete package for aerosol impact at high spatial resolution (Landsat, S2,AERONET,CAMSIS,SKYCAM).